

## Calculation of Output Optical Signals of Mechanoluminescent Impulse Pressure Sensors

**Konstantin TATMYSHEVSKIY**

Vladimir State University, 87 Gorky Str., 600000, Vladimir, Russia

Tel.: + 79051456012, fax: + 7(4922)335242

E-mail: [tatmysh@vlsu.ru](mailto:tatmysh@vlsu.ru)

*Received: 30 August 2019 / Accepted: 27 September 2019 / Published: 30 November 2019*

---

**Abstract:** Mechanoluminescence is the visible or infrared radiation of solids arising from mechanical action. The brightest glow is observed under the influence of pulsed pressures. Mechanoluminescent sensors are based on the principle of direct conversion of the input mechanical pressure into the output optical signal. Such sensors can be used in conjunction with fiber optic data transmission channels, which provides high noise immunity to electromagnetic interference. This article describes the physical mechanism of operation of mechanoluminescent sensors made of ZnS:Mn. Mechanoluminescence occurs upon excitation of luminescence centers in the form of atoms Mn due to the displacement of charged dislocations accompanying the plastic deformation of the sensor. The mathematical model of the sensor and the results of calculating the output optical signals depending on the parameters of the pressure pulses are presented.

**Keywords:** Mechanoluminescence, Mechanoluminescent sensor, Dislocation kinetics, Light generation sensor.

---

### 1. Introduction

Pressure control and monitoring is required in various situations. Often, pressure measurement is necessary in the so-called extreme conditions in which the measuring circuit is exposed to the powerful effects of electromagnetic interference and ionizing radiation. In addition, in traditional measuring systems, cable lines can themselves serve as sources of interference, as well as be potentially unreliable in conditions of increased spark and explosion hazard. Currently, fiber-optic data acquisition systems are being intensively developed [1-4]. Fiber-optic communication lines (FOCL) have a number of fundamental advantages that stimulate their use in information-measuring systems (IMS) operating in extreme conditions:

- Lack of crosstalk of adjacent channels; high load-bearing ability, allowing to build branched systems;

- Immunity to electromagnetic interference, high temperature, radiation;

- Small weight and dimensions;

- Electrical contactlessness, galvanic isolation of the receiver and signal source; unidirectional flow of information and the lack of response of the photodetector to an optical radiation source; the impossibility of short circuits, arcing and the elimination of the need for grounding.

The use of traditional electronic sensors as part of electromagnetic noise-protected IMS with fiber-optic channels requires the supply of power to them via an additional electric wire line, as well as the presence of a converter of the non-optical information signal of such a sensor into an optical one and matching devices with a fiber-optic channel. All this, taking into account the errors of the electric sensors themselves, reduces the level of noise immunity and accuracy of the IMS, increases their size and weight. Therefore, for IMS

with fiber-optic communication channels, it is preferable to use parametric and generator sensors that use signals of the same physical nature in their work as optical fibers, that is, optical [1, 3-4].

Mechanoluminescent light-generating pressure sensors fully correspond to the fulfillment of the second condition. Here, the use of output light signals solves the problems of pairing sensors with FOCLs and increasing the noise immunity to electromagnetic interference, the absence of moving parts, the solidity and planarity of the sensing element provide reliability, and the use of its spatial modulation in addition to the amplitude-time parameters of the optical signal, various spectra and polarization states increases the information content.

Mechanoluminescent sensors (MLS) are based on the principle of direct conversion of the mechanical energy of an elastoplastic deformation into the energy of optical radiation, which is recorded by a photodetector [5]. Structurally, MLS is a thin-layer element, which includes fine crystalline phosphor powder (ZnS:Mn) and a transparent binding material. Mn atoms play the role of luminescence centers (LC) in these sensors [6-7]. The optimum thickness of the MLS does not exceed 20...100 μm, which is determined by the particle size distribution of the powder and the characteristics of light propagation in fine powder layers. Film MLS in conjunction with a matrix photodetector allows you to visualize and record impulse pressure fields [8].

Such sensors can be used, for example, to control the operation of automotive airbags, as sensors for structural damage, planar sensors for visualizing impulsive pressure fields [9-11].

## 2. Mechanoluminescent Sensor

### 2.1. Block Diagram of an Information Circuit with MLS

A generalized block diagram of the information circuit of a measuring device with a MLS is shown in Fig. 1.

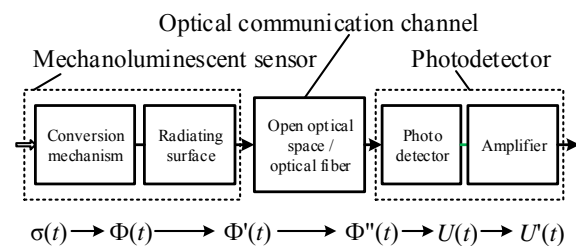


Fig. 1. Generalized block diagram of energy conversion in the information circuit of a recording device with MLS.

The scheme corresponds to the structure of a conventional optocoupler and includes a MLS, a photodetector, and an optical communication channel between them.

Here, the pressure (mechanical stress)  $\sigma(t)$  acts at the sensor input, causing deformation of the phosphor crystals. Under the action of deformation, the luminescent material is excited and generates a light pulse  $\Phi(t)$ . Since the radiating surface of the MLS has a fine-grained structure, and the phosphor crystals are opaque, only part of the total generated radiation energy will act at the output of the MLS. Depending on the ratio of the sizes of the luminous region and the input aperture of the optical medium, only part of the radiation  $\Phi'(t)$  can be introduced into it. Losses within the optical medium are characterized by transmittance. At the exit from it and, accordingly, on the receiving surface of the photodetector, the light flux  $\Phi''(t)$  will act. With the known sensitivity of the photodetector, the voltage at its output will be  $U(t)$ , which is then amplified by a pre-normalizing (normalizing) amplifier to the value  $U'(t)$ . Further, the signal can be fed to a processing unit or a computer, where it is subjected to analog-to-digital conversion and subsequent digital processing according to a predetermined algorithm.

The values of gain, photosensitivity, and transmittance (loss coefficient) of the optical medium, as a rule, are known for various components of the information circuit. Therefore, in order to calculate the output optical signals of the MLS, it is first necessary to determine: 1) how is the conversion of mechanical energy to radiation energy; 2) what parameters of the output optical signal are informative and how they are functionally related to the parameters of the input pressure pulse; 3) how efficiently the optical radiation is removed from the sensitive element to the optical communication channel.

### 2.2. MLS Design Requirements

The conversion coefficient of the optoelectronic circuit with MLS as the ratio of the voltage at the output of the photodetector to the input pressure at the input of the sensor is determined by the equation:

$$K_{conv} = \Phi(\sigma) \eta_{out} \eta_{OCC} \eta_{in} S_{\lambda} K_{Amp}$$

where  $\Phi(\sigma)$  is the conversion function connecting the input pressure and the output light flux;  $\eta_{out}$  is the coefficient of radiation output from the surface of the MLS to the optical communication channel;  $\eta_{OCC}$  is the coefficient of radiation loss in the optical communication channel;  $\eta_{in}$  is the input coefficient of radiation from the optical communication channel to the photodetector;  $S_{\lambda}$  is the sensitivity of the photodetector in the band of the spectrum of ML radiation;  $K_{Amp}$  is the amplifier gain.

To achieve high values  $K_{conv}$ , it is necessary to use highly efficient components. The requirements for the photodetector in terms of detection ability, sensitivity and fast action, and for the amplifier in terms of the slew rate of the output voltage and gain. It is necessary

to maximize the coupling of the emitter and the photodetector according to the spectral characteristics, and also to minimize radiation losses in the optical communication channel [1, 4].

The main prerequisites for the development of measuring devices with MLS is the knowledge of the conversion function  $\Phi(\sigma)$  and the provision on the basis of this knowledge of high levels of radiation flux when exposed to a pressure sensor that is characteristic of the actual operating conditions of the product. Knowing the conversion function and the radiation spectrum makes it possible to most efficiently construct the photodetector scheme, as well as calculate the parameters of the MLS and other sensor elements. It should be noted that in contrast to photoluminescence and cathodoluminescence, mechanoluminescent properties characterize both the applied mechanoluminophore and the sensor design. This is due to the pulsed mechanical nature of the inlet pressure effect on the MLS. Therefore, the output radiation flux largely depends on whether it is possible in this hypothetical design to efficiently transfer mechanical energy to a sensitive element.

The basic requirements for the MLS design can be formulated as follows:

- The design must ensure the supply of energy of the pressure pulse to the MLS and the output of radiation from the surface of the MLS to the optical communication channel;

- The sensitive element should give out a radiation pulse with an amplitude and duration that ensure reliable recording in a given range of input actions;

- The output optical signal must have informative parameters (parameter), which allow unambiguous determination of the main parameters of the input pressure pulse  $\sigma(t)$ .

Due to the fact that the MLS is actually an emitter with mechanical excitation, its main properties can be described by the characteristics and parameters used to describe the properties of emitters.

### 2.3. ML Sensor Structure

The optical parameters of a mechanoluminescent sensitive element that determine the radiation transfer in it, primarily depend on its structure. In the most common simplest case, the MLS structure is a plane-parallel light-scattering layer of particles of powdered luminescent material in a solidified transparent binder. Such a layer is applied to a substrate made of a transparent material, which ensures, firstly, the creation of the stress state of the particles during the propagation of a pressure impulse (a wave of mechanical stresses) through the layer, and secondly, the radiation is removed to a photodetector. Epoxy, melamine-formaldehyde and other resins, varnishes, polystyrene and other transparent materials are used as a binder for powder phosphors. Plates from various glasses, optical ceramics, fiber optic bundles and cables, foci can be used as a substrate.

Fig. 2 shows the structure MLS. The sensitive element of the sensor is a thin film of a hardened suspension of luminescent powder in a transparent binder.

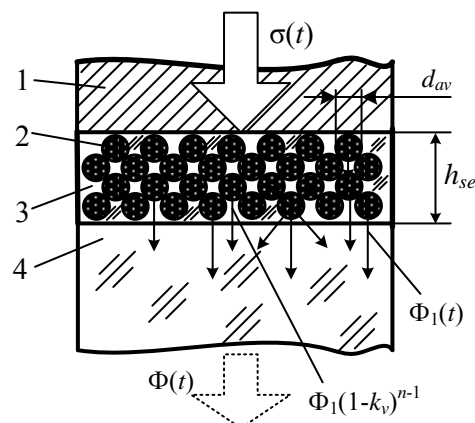


**Fig. 2.** The structure of the sensitive element of the MLS: 1 - Pressure transmission element; 2 - Phosphor particles; 3 - Transparent binder material; 4 - Transparent substrate.

The optical parameters of the MLS, which determine the transfer of radiation in it, primarily depend on its internal structure. The most significant parameter of MLS is the thickness of the sensitive element. The thickness of the layer, the volume concentration of the powder particles in it, and the weight concentration of the dopant that creates the LC determine the total number of  $N_{LC}$  participating in the radiation process. Conventionally, individual particles of the phosphor can be considered balls of the same diameter, uniformly located on the surface of the substrate and not overlapping each other. We call such a single-row layer of particles a monolayer. For a layer of  $n$  with such layers, the volume packing coefficient  $k_v$ , which is equal to the ratio of the volumes of all particles to the volume of the layer, is limited to 0.86. Actually achieved values of  $k_v$  usually lie in the range  $0.3 \leq k_v \leq 0.73$ .

The total flux of MLS radiation increases with an increase in the number of particles in a monolayer and with an increase in the number of monolayers, however, an increase in the flux reaches saturation, since with a sufficiently large number of monolayers the luminescence of deeply lying layers is completely scattered by the overlying layers. The transparency of a single monolayer can be taken equal to  $(1-k_v)$ . Thus, it is assumed that a single particle transmits only its radiation and is opaque to radiation from underlying particles, and the radiation passes only in the gaps between the particles. Denoting the radiation flux of the monolayer  $\Phi_1(t)$  closest to the substrate, we determine the total flux from the sensitive element with a thickness  $h_{se}$ :

$$\Phi(t) = \Phi_1(t) [1 + \sum_{i=1}^n (1-k_v)^i] = \Phi_1(t) k_n, \quad (1)$$

where  $n = h_{se}/d_{av}$  - number of layers;  $d_{av}$  is the average particle diameter of the phosphor;  $i$  is the number of layers except the first;  $k_n$  is the coefficient of unevenness of the contribution of the glow of the layers. This equation makes it possible to bring the total radiation flux  $\Phi(t)$  to the flux of the first monolayer  $\Phi_1(t)$ , and to take into account the non-uniformity of the contribution of the remaining layers to the total flux using the luminance unevenness coefficient  $k_n$ . An analysis of Eq. (1) shows that the optimal number of layers is  $n = 3 \dots 6$ , since their further increase will give an increase in luminous flux of not more than 5 %.

A separate MLS monolayer emits a stream within the full solid angle. In this case, only half of the total flux comes out in the direction of the photodetector, the second half is scattered by the underlying layers and does not enter the photodetector, which is taken into account by the coefficient  $k_\Omega = 0.5$ .

The radiation losses that occur when the MLS radiation is introduced into the optical communication channel must be taken into account by the additional radiation input coefficient  $k_{in}$ . Thus, taking into account the design parameters and the internal structure of the sensitive element, the total flux of radiation output from the site to the optical channel can be found as  $\Phi(t) = 0.5 k_{in} k_n \Phi_1(t)$ .

### 3. Mathematical Model

#### 3.1. Mechanoluminescence Mechanism

It has been shown that mechanoluminescence (ML) in crystalline compounds is a consequence of the processes of motion of dislocations that accompany the plastic deformation in crystals [12]. Dislocations in  $A_2B_6$  semiconductors, and in particular ZnS, have a strong electrical charge. In the process of plastic deformation, LC interacts with the electric field of moving charged dislocations, which leads to the excitation of LC with their subsequent radiative transitions.

The physical model of ML is based on the phenomenon of tunneling of electrons in impurity LC in an electric field of moving dislocations arising from plastic deformation of a crystal [12]. During plastic deformation, the dislocations begin to move within the volume of the crystal. While the plastic deformation continues, excitation processes of LC prevail. After its termination, an exponential decrease in luminescence is observed due to the transition of excited LC to the stationary state.

#### 3.2. Radiation Kinetics Equation

The specific flux of optical radiation in MLS is determined by the equation:

$$\Phi(t) = \frac{\eta}{\tau} \exp\left(-\frac{t}{\tau}\right) \int_0^{t_\sigma} N_{LC} 2r_{in}(t) \tilde{N}_{mD}(t) \tilde{V}_D(t) dt, \quad (2)$$

where  $\eta$  is the energy of a light quantum;  $\tau$  is the time constant corresponding to the exponential attenuation of the intracenter mechanoluminescent characteristic of Mn atoms;  $t_\sigma$  is the pressure pulse duration time;  $N_{LC}$  is the total number of LC in the sensor;  $r_{in}(t)$  is the interaction radius of a moving dislocation with LC;  $\tilde{N}_{mD}(t)$  is the average density of mobile dislocations;  $\tilde{V}_D(t)$  is the average dislocation velocity. Here, the integrand describes the kinetics of excitation of LC during the action of the pressure pulse  $t_\sigma$ , and the equation before the integral describes the kinetics of luminescence attenuation.

#### 3.3. Sensor Deformation Equation

The kinetics of excitation depends on plastic strain  $\varepsilon_p$ , the speed of which is determined by the Orowan equation [13]:

$$\dot{\varepsilon}_p = |\vec{b}| \tilde{N}_{mD}(t) \tilde{V}_D(t), \quad (3)$$

where  $|\vec{b}|$  is the modulus of the Burgers vector characterizing the lattice distortion by the dislocation. The stress-strain state of MLS for the case of uniaxial application of pressure is determined by the equation:

$$\sigma_1 = E \left( \varepsilon_1 - \frac{4}{3} \varepsilon_p \right) = \sigma(t) - E \varepsilon_{1p}, \quad (4)$$

where  $\sigma_1$  is the principal stress applied perpendicular to the MLS plane,  $E$  is the Young's modulus,  $\varepsilon_1$  is the total strain in the form of the sum of the elastic  $\varepsilon_{1e}$  and plastic  $\varepsilon_{1p}$  components,  $\sigma(t)$  is the pressure pulse. Eq. (4) shows that stresses increase with an increase in total strain  $\varepsilon_1$ , and decrease due to plastic  $\varepsilon_{1p}$ . Here the case of quasistatic deformation, i.e. observance of uniformity of plastic deformations across the thickness of the MLS was considered. This condition is fulfilled either at low strain rates or at small ratios of the thickness of the sensor to its diameter.

Dislocation parameters are found by Gilman equations [14]

$$\tilde{N}_{mD} = \tilde{N}_{tD} \exp\left(-\frac{\tilde{N}_{tD}}{\tilde{N}_{tcr}}\right), \quad (5)$$

$$\tilde{N}_{tD} = \tilde{N}_{tD0} + M \varepsilon_p, \quad (6)$$

where  $\tilde{N}_{tD}$  is the average total dislocation density;  $\tilde{N}_{tcr}$  is the critical value of the total dislocation density corresponding to the end of the yield area in the  $\sigma(\varepsilon)$  diagram,  $\tilde{N}_{tD0}$  is the initial value of the total density of dislocations;  $M$  is the dislocation multiplication factor.

The average dislocation velocity can be determined by the Eq. [14]:

$$\tilde{V}_D(t) = k_s c_{tr} \exp\left(\frac{D_f}{\sigma_1}\right), \quad (7)$$

where

$$k_s = \begin{cases} 0, & \text{if } \sigma_1 < \sigma_S; \\ 1 - 2 \frac{\exp[0,5(\sigma_S - \sigma_1)]}{\sigma_1 - \sigma_S}, & \text{if } \sigma_1 > \sigma_S, \end{cases}$$

$k_s$  is the correction factor, zeroing the speed of dislocations at pressures below the yield strength;  $c_{tr}$  is the shear wave velocity in the crystal;  $D_f$  is the effective stress of internal friction;  $\sigma_S$  is the static yield strength. The average velocity of dislocations in the Eq. (3) is very sensitive to shear stresses in the slip plane and in the limit can reach values of  $c_{tr}$ . However, in the region close to the limit of static yield stress, the Eq. (7) must be corrected, since it does not take into account the existence of a threshold value of the yield stress below which dislocation motion does not occur. This threshold value is determined by the existence of the so-called Peierls-Nabarro barrier [15] and is associated with a static yield strength  $\sigma_S$ . Therefore, in the region of low stresses  $\sigma_1 < \sigma_S$ , the correction coefficient  $k_s$  is introduced into dependence (7), which does not change  $\tilde{V}_D$  if  $\sigma_1 < \sigma_S$  and decreases  $\tilde{V}_D$  at  $\sigma_1 > \sigma_S$ .

### 3.4. Settlement Conditions

Modeling of the light flux arising when a mechanoluminescent sensing element is excited by a pressure pulse is performed in MATLAB. The program determines the quantum-mechanical, electrical and kinetic characteristics of the mechanoluminescent material based on the industrial electroluminophore ELS-580C.

The mathematical model is a system of integro-differential Equations (2) and (3). The ode113 function was chosen from the MATLAB function library to solve the ordinary differential equation. Is a solver of variable order based on the formula of Adams - Bashforth - Moulton. It can be more effective than the usual Runge-Kutta method of the 4<sup>th</sup> and 5<sup>th</sup> order at high requirements to accuracy and in cases when the complexity of calculating the right parts is high. It is a multi-step solver that requires knowing the solutions at several preceding points to compute the solution at the current point.

To calculate a certain integral, the Quadra-tour - quad method was chosen. Quadrature is a numerical method for calculating the area under a function graph. The function quad ('fun', a, b) returns the numerical value of a certain integral from a given function 'fun' on the segment [a b]. The adaptive Simpson method is used.

ELS-580C industrial electroluminophore (composition - ZnS:Mn, Cu; weight-percent manganese content of 1%) was chosen as the mechanoluminescent material in the calculations. The

reasons for choosing this particular material for theoretical and experimental studies were as follows:

- Zinc sulfide phosphors activated by manganese have the brightest luminescence under mechanical stress;

- The maximum of the emission spectrum corresponds to the yellow-orange glow and is more consistent with the maximum spectral sensitivity of modern high-speed silicon photodetectors;

- This electroluminophore is produced by the industry in series. Therefore, its physical, chemical and mechanical properties are quite reproducible and a priori known.

The latter circumstance can be recognized as very important, since the results of numerous studies [4-5, 8-11, 16] show contradictory results, which are not only inconsistent with each other, but also differ within the framework of one experimental study [7]. One explanation for such discrepancies may be the fact that the researchers did not control both the actual dislocation structure of crystalline samples and the history of their mechanical loading. Analysis of Eqs. (5) and (6) shows that the initial dislocation density  $\tilde{N}_{ID0}$  and its relation to the critical density  $\tilde{N}_{tr}$  have a very strong effect on the density of mobile dislocations  $\tilde{N}_{mD}$ , which largely determines the intensity of mechanoluminescent radiation.

To determine the magnitude of the Burgers vector, an assumption was made that the material is a single spherulite structure. In the calculations, only the energy of radiation quanta corresponding to the maximum of the emission spectrum of manganese emission centers ( $\lambda=580$  nm;  $\eta=3.52 \cdot 10^{-19}$  J) was taken into account, since the radiation intensity of copper LCs is approximately 50 times weaker [17-19].

The parameters of the dislocation structure of the phosphor were determined taking into account the production technology of luminescent powders. In the performed calculations, the values  $k_{in}=1$ ,  $n=2$ ,  $d_{av}=10$   $\mu$ m,  $k_v=0.6$ , and  $k_n=1.4$  were taken. These values were chosen because they corresponded to the fabricated experimental MLS samples.

The luminescence decay kinetics corresponds to intracenter luminescence [18], characteristic of ZnS: Mn, with a time constant  $\tau = 150$   $\mu$ s. The energy luminosity of the MLS  $R(t)=0.5k_{in}k_n\Phi_1(t)$  was calculated, i.e., the flow power emitted by a unit surface area equal to 1 mm<sup>2</sup> was calculated.

### 3.5. Key Model Assumptions

When constructing a mathematical model of a mechanoluminescent sensing element, the following basic assumptions were made:

- 1) Only one type of luminescence centers (Mn) are involved in the formation of radiation, which generate light quanta with a fixed energy;

- 2) The probability of tunneling is equal to one;

- 3) The centers of luminescence are evenly distributed inside the crystal;

- 4) All phosphor crystals have the same crystalline structure;
- 5) Individual particles of the phosphor inside the layer of the sensing element are distributed randomly;
- 6) The dislocation structure in all particles of the same phosphor;
- 7) Mobile dislocations can excite each center of luminescence during the duration of a pressure pulse only once;
- 8) The dislocation charge does not depend on the strain rate;
- 9) Radiation is removed from the sensitive element into only one hemisphere, and part of the radiation sent to another hemisphere is completely absorbed and scattered inside the element;
- 10) Phosphor particles are evenly distributed over the area of the sensitive element.

### 3.6. Calculation Results

The input action was described by a single pressure pulse having a half-sinusoidal shape  $\sigma(t) = \sigma_A \sin(\pi t / t_\sigma)$ . Such a pulse shape is closest to pressure pulses arising in real structures.

The nature of the change in the output optical signals of the sensitive element with a change in amplitude, but with a constant duration of pressure pulses, is shown in Fig. 3.

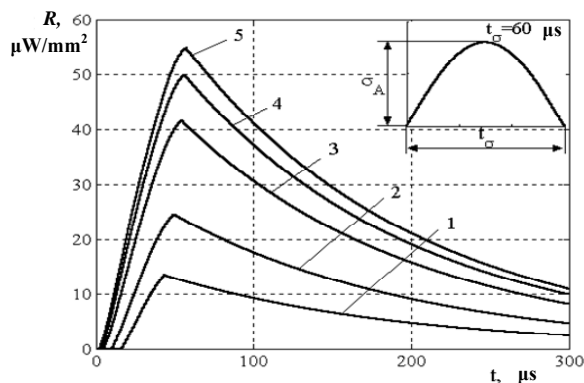


**Fig. 3.** Estimated dependences of an energy luminosity  $R(t)$  of MLS under an influence of pressure impulses of identical duration  $t_\sigma = 60 \mu\text{s}$  and varying amplitude  $\sigma_A$ :  
 1 -  $\sigma_A = 60 \text{ MPa}$ ; 2 -  $\sigma_A = 90 \text{ MPa}$ ; 3 -  $\sigma_A = 180 \text{ MPa}$ ;  
 4 -  $\sigma_A = 270 \text{ MPa}$ ; 5 -  $\sigma_A = 360 \text{ MPa}$ .

It can be seen here that with decreasing amplitude and, accordingly, the steepness of the pressure pulse, an increase in the time delay in the appearance of radiation is observed. The time delay is determined by the time the input pulse reaches a pressure value equal to the yield strength of the material of the sensing element. This emphasizes the threshold character of the conversion function of mechanoluminescent sensors. Within the framework of the developed model, it is believed that, within the limits of elastic deformations, radiation generation practically does not occur. Experimental studies have shown that

mechanoluminescent radiation is observed even at pressures slightly lower than the yield strength. However, its intensity is several orders of magnitude lower, and the flare structure in the form of separate short bursts of light differs significantly from the considered one and cannot be reproduced by the developed model.

In addition, there is a time shift between the maximum pressure in the pulse and the maximum radiation, and the shift has a small increase with increasing amplitude of the pressure impulse.

The nature of the change in the output optical signals of the sensing element with a change in the pressure pulse duration, but with a constant amplitude, is shown in Fig. 4.

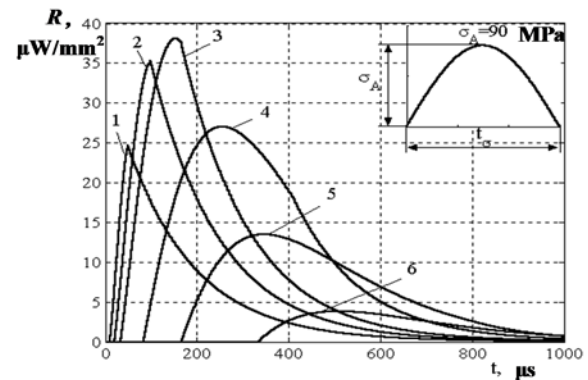


**Fig. 4.** Estimated dependences of the energy luminosity  $R(t)$  under the action of pressure impulses of the same amplitude  $\sigma_A = 90 \text{ MPa}$  and different duration  $t_\sigma$ :  
 1 -  $t_\sigma = 60 \mu\text{s}$ ; 2 -  $t_\sigma = 120 \mu\text{s}$ ; 3 -  $t_\sigma = 200 \mu\text{s}$ ;  
 4 -  $t_\sigma = 500 \mu\text{s}$ ; 5 -  $t_\sigma = 1000 \mu\text{s}$ ; 6 -  $t_\sigma = 2000 \mu\text{s}$ .

It can be seen here that with a monotonic increase in the duration, the luminosity amplitude first increases, and then, after reaching a maximum, the intensity of the luminescence pulse decreases. This process is accompanied by a significant change in the shape of the radiation pulse. If in the range of durations of input pressure pulses  $t_\sigma \approx 20 \dots 200 \mu\text{s}$  the glow pulses had a sharp peak and a fairly steep leading edge, then in the range of durations of pressure pulses  $t_\sigma \approx 200 \dots 2000 \mu\text{s}$  the glow pulses sharply decrease in magnitude, the duration of the front and trailing fronts become almost the same.

In addition, a temporal shift is observed between the maximum pressure in the pulse and the maximum of the radiation, and the magnitude of the shift has a significant increase with increasing duration of the pressure pulse and, accordingly, the duration of loading.

This is explained by the fact that two competing processes simultaneously occur during the process of generating mechanoluminescent radiation.

The essence of the first process is that in the mechanoluminescent crystals, the accumulation of excited luminescence centers occurs at different rates. The rate of their accumulation depends mainly on the rate of application of pressure. The essence of the



second process is the return of the excited glow centers to the initial state, which is accompanied by the emission of light quanta (luminescence). The second process has a constant speed, which is described by the law of the mono-molecular reaction (exponential attenuation).

Accordingly, if the excitation rate is much higher than the return velocity, then intense mechanoluminescence with a steep rise front will be observed. In the opposite case, the concentration of excited centers of luminescence will not be enough for noticeable radiation to appear. Such a process will occur even despite the fact that the total deformation of the phosphor of the sensing element can be significantly greater than at high loading speeds. This manifests itself repeatedly noted by various researchers, a significant sensitivity of the intensity of mechanoluminescence to the speed of mechanical loading.

#### 4. Conclusions

A mathematical model of MLS based on zinc sulfide phosphor doped with manganese has been developed. The model is based on a clear interpretation of the physical processes leading to mechanoluminescence. The developed methodology for calculating the output optical signals of the MLS allows us to determine the magnitude of the signal in absolute units of light flux. The model takes into account the design features of the MLS. The results are in good agreement with experimental data [20].

The calculation results show that, firstly, the MLS conversion function has a pronounced sensitivity threshold, secondly, the conversion function has a substantially nonlinear character, and thirdly, the shape of the output optical signals differs significantly from the shape of the input pressure pulses.

Comparison of the obtained results with the data of modern semiconductor photodetectors showed that reliable detection of the optical MLS signal is possible for further processing. The results were presented briefly at the conference [21].

#### References

- [1]. E. Udd (Editor), *Fiber Optic Sensors: An Introduction for Engineers and Scientists*, 2<sup>nd</sup> Edition, Wiley-Interscience, New York, NY, 2006.
- [2]. J. Fraden, *Handbook of Modern Sensors: Physics, Designs and Applications*, 5<sup>th</sup> Edition, Springer, New York, 2016.
- [3]. R. J. Jackson, *Novel Sensors and Sensing*, CRC Press, Boca Raton, 2004.
- [4]. D. O. Olawale, T. Dickens, W. G. Sullivan, O. I. Okoli, J. O. Sobanjo, B. Wang, Progress in triboluminescence-based smart optical sensor system, *Journal of Luminescence*, Vol. 131, Issue 7, 2011, pp. 1407-1418.
- [5]. B. P. Chandra, «Mechanoluminescence», in *Luminescence of Solids*, Edited by D. R. Vij, Plenum Press, New York, 1998, pp. 361-389.
- [6]. L. Kobakhidze, C. J. Guidry, W. A. Hollerman, R. S. Fontenot, Detecting Mechanoluminescence from ZnS:Mn Powder Using a High Speed Camera, *IEEE Sensors Journal*, Vol. 13, Issue 8, 2013, pp. 3053-3059.
- [7]. Chao-Nan Xu, Xu-Guang Zheng, Tadahiko Watanabe, Morio Akiyama, Ichiro Usui, Enhancement of adhesion and triboluminescence of ZnS:Mn films by annealing technique, *Thin Solid Films*, Vol. 352, Issue 1-2, 1999, pp. 273-277.
- [8]. V. K. Chandra, B. P. Chandra, Dynamics of the mechanoluminescence induced by elastic deformation of persistent luminescent crystals, *Journal of Luminescence*, Vol. 132, Issue 3, 2012, pp. 858-869.
- [9]. I. Sage, G. Bourhill, Triboluminescent materials for structural damage monitoring, *Journal of Materials Chemistry*, Vol. 11, Issue 2, 2001, pp. 231-245.
- [10]. N. P. Bergeron, W. A. Hollerman, S. M. Goedeke, M. Hovater, W. Hubbs, A. Finchum, R. J. Moore, S. W. Allison, D. L. Edwards, Experimental evidence of triboluminescence induced by hypervelocity impact, *International Journal of Impact Engineering*, Vol. 33, Issue 1-12, 2006, pp. 91-99.
- [11]. A. Feng, S. Michels, A. Lamberti, P. F. Smet, Mechanoluminescent materials: a new way to analyze stress by light, in *Proceedings of the 18<sup>th</sup> International Conference on Experimental Mechanics (ICEM'18)*, Brussels, Belgium, 1-5 July 2018, Vol. 2, Issue 8, 492.
- [12]. Yu A. Ossipian, *et al.*, Electronic properties of dislocations in semiconductors, *Editorial USSR*, Moscow, 2000.
- [13]. J. W. Taylor, Dislocation dynamics and dynamic yielding, *Journal of Applied Physics*, Vol. 36, Issue 10, 1965, pp. 3146-3150.
- [14]. J. J. Gilman, Dislocation dynamics and response of materials to impact, *Applied Mechanics Reviews*, Vol. 21, Issue 8, 1968, pp. 767-783.
- [15]. J. P. Hirth, J. Lothe, *Theory of Dislocations*, Wiley-Interscience Publication, Toronto, 2<sup>nd</sup> Edition, 1982.
- [16]. W. A. Hollerman, R. S. Fontenot, K. N. Bhat, M. D. Aggarwal, C. J. Guidry, K. M. Nguyen, Comparison of triboluminescent emission yields for 27 luminescent materials, *Optical Materials*, Vol. 9, 2012, pp. 1521-1547.
- [17]. P. Thiessen, K. Meyer, Tribolumineszenz bei Verformungs fester Körper, *Naturwissenschaften*, Vol. 9, 1970, pp. 423-427.
- [18]. L. Sodomka, *Mechanoluminescence a její pouziti*, Academia, Praha, 1985, 226 p.
- [19]. B. P. Chandra, M. S. Khan, M. H. Ansari, Cleavage Mechanoluminescence in Crystals, *Crystal Research and Technology*, Vol. 33, Issue 2, 1998, pp. 291-302.
- [20]. N. Yu. Makarova, K. V. Tatmyshevskiy, A table for experimental study of mechanoluminescent pulse pressure transducers, *Instruments and Experimental Techniques*, Vol. 49, Issue 1, 2006, pp. 135-140.
- [21]. K. Tatmyshevskiy, Mechanoluminescent pulse pressure sensors, in *Proceedings of the 5<sup>th</sup> International Conference on Sensors Engineering and Electronics Instrumentation Advances (SEIA'19)*, Tenerife (Canary Islands), Spain, 25-27 September 2019, pp. 182-184.



**Universal Frequency-to-Digital Converter  
(UFDC-1 and UFDC-1M-16)  
in MLF (5 x 5 x 1 mm) package**

**SMALL WORLD -  
BIG FEATURES**

SWP, Inc., Toronto, Ontario, Canada,  
Tel. + 34 696067716, fax: +34 93 4011989, e-mail: sales@sensorsportal.com  
[http://www.sensorsportal.com/HTML/E-SHOP/PRODUCTS\\_4/UFDC\\_1.htm](http://www.sensorsportal.com/HTML/E-SHOP/PRODUCTS_4/UFDC_1.htm)



**Universal Sensors and Transducers Interface  
(USTI-EXT) for extended temperature range**

**-55 °C ... +150 °C**

26 measuring modes for all frequency-time parameters,  
rotational speed, capacitance Cx, resistance Rx, resistive bridges  
Frequency range, 0.05 Hz ... 7.5 MHz (120 MHz);  
Programmable relative error, % 1 ... 0.0005 %  
Conversion speeds 6.25 us ... 12.5 ms  
SPI, I2C, RS232 (master and slave, up to 76 800 baud rate)  
Packages: 32-lead, 7x7 mm TQFP and 32-pad, 5x5 mm (QFN/MLF)

**Applications: automotive industry, avionics, military, etc.**

<http://excelera.io/>      [info@excelera.io](mailto:info@excelera.io)

